SCIENCE CHINA
Technological Sciences

February 2013 Vol.56 No.2: 423–429
doi: 10.1007/s11431-012-5065-5

Pendulum-like oscillation controller for micro aerial vehicle with ducted fan based on LQR and PSO

DUAN HaiBin[1,2*] & SUN ChangHao[2]

[1] *State Key Laboratory of Virtual Reality Technology and Systems, Beihang University, Beijing 100191, China;*
[2] *Science and Technology on Aircraft Control Laboratory, Beihang University, Beijing 100191, China*

Received August 13, 2012; accepted October 7, 2012; published online November 20, 2012

This paper describes a novel type of pendulum-like oscillation controller for micro air vehicle (MAV) hover and stare state in the presence of external disturbances, which is based on linear-quadratic regulator (LQR) and particle swarm optimization (PSO). A linear mathematical model of pendulum phenomenon based upon actual wind tunnel test data representing the hover mode is established, and a hybrid LQR and PSO approach is proposed to stabilize oscillation. PSO is applied to parameter optimization of the designed LQR controller. A series of comparative experiments are conducted, and the results have verified the feasibility, effectiveness and robustness of our proposed approach.

micro air vehicle (MAV), pendulum-like oscillation, linear-quadratic regulator (LQR), particle swarm optimization (PSO)

Citation: Duan H B, Sun C H. Pendulum-like oscillation controller for micro aerial vehicle with ducted fan based on LQR and PSO. Sci China Tech Sci, 2013, 56: 423–429, doi: 10.1007/s11431-012-5065-5

1 Introduction

Micro aerial vehicle (MAV) offers several advantages as one type of autonomous uninhabited aerial vehicles (UAVs). They can be very small with a compact layout. Many are capable of high-speed flight in addition to the normal hover and vertical takeoff and landing capabilities. These features make them well suited for a variety of missions, especially in urban environments [1]. A recent US government's announcement of plans to greatly increase the number of unmanned aircraft on stations in Iraq and Afghanistan drives the surge in interest for unmanned vehicles. Prof. Robert [2], who is the US Defense Secretary, commented that unmanned aircraft are essential to provide real-time video of insurgent activity and argued that the need is growing at 300 percent per year. Nowadays, many companies are working towards research and development of MAVs, and the representative achievements are Cypher series by Sikorsky and MAVs by Honeywell etc. [3]. As for issues such as control law designs, navigation approaches and aerodynamics analysis of MAVs, researchers all over the world have been devoting all their efforts and considerate findings have been achieved. Bio-inspired intelligence provides a new way for controller design [4], and Duan [5, 6] applied several bio-inspired computation algorithms to UAV's controller designs. Christian [7] proposed the natural feature method for vision based navigation of a MAV. Tsai [8] successfully designed a flapping-wing MAV, and its aerodynamics was also analyzed; Thomas [9] designed a simple, nonlinear closed-loop control law for the dynamics along the vertical and pitch axis of a flapping-wing MAV, allowing an efficient stabilization of the naturally unstable model. Pflimlin [10] studied the aerodynamic modeling of a ducted fan vertical takeoff and landing (VTOL) UAV and the problem of attitude stabilization when the vehicle is remotely controlled by a pilot in presence of crosswind. Pu [11, 12] designed and imple-

*Corresponding author (email: hbduan@buaa.edu.cn)

mented a novel type of VTOL UAV. Osgar [13] gave the presentation of a new non-dimensional modeling scheme with an in-depth analysis discussion of its implications.

Hover and stare are of the paramount importance to the performance of MAVs, as they are designed to perform surveillance and reconnaissance missions. However, pendulum-like oscillation (see Figure 1) triggered by external disturbances and other uncertain factors will badly impair its performance, resulting in blurred images, even MAVs' overturning. As a result, with their wide applications in civil and military fields, control techniques for MAVs with regard to the hover and stare state are becoming more and more important for better performances of surveillance and reconnaissance missions. This work focuses on a particular kind of MAV, which is driven by a rotor and a ducted-fan, and proposes a combination control law design approach to stabilize the hover and stare pendulum-like oscillation based on linear-quadratic regulator (LQR), in which an improved particle swarm optimization (PSO) algorithm is utilized for parameter optimization of matrixes $\boldsymbol{Q}$ and $\boldsymbol{R}$ in the linear quadratic regulator. In this way, the MAV's dynamic properties can be ameliorated efficiently while executing surveillance missions that requires perfect stability and rapid responses.

The rest of this paper is organized as follows. Section 2 introduces the mathematical model of the MAV pendulum-like oscillation. Subsequently, a hybrid LQR controller based on PSO is developed in Section 3, and a series of experiments are conducted in Section 4. Our concluding remarks are in Section 5.

2 Mathematical model of MAV pendulum-like oscillation

The MAV in this work adopts the axial symmetrical layout. Owing to the fact that the suspension centre moves freely with rotor wings in the plane [10, 11], the pendulum-like oscillation is non-linear, strongly coupled and of high order [12]. In this section, a mathematical model representing the pendulum-like oscillation in the hover and stare state is obtained by using the Lagrangian method, and the corresponding linearized model is obtained in the neighborhood of the hover and stare equilibrium.

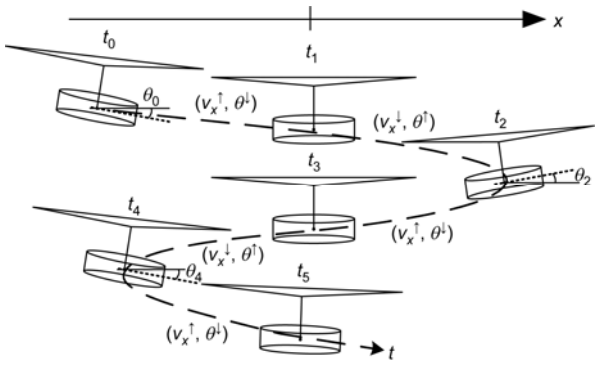

Figure 1 Pendulum-like oscillation in actual flight (x-axis).

2.1 Nonlinear mathematical model of MAV pendulum-like oscillation

The pendulum can be abstracted as a system consisting of the suspension point O_h, the pendulum rod O_hO_t and the pendulum mass O_t (see Figure 2).

In Figure 2, the $OXYZ$ is the ground-fixed coordinate system, the $O_hx_1y_1z_1$ represents a mobile ground coordinate system, with point O_h being the origin and parallel to the $OXYZ$, while the $O_hx_2y_2z_2$ is defined as the pendulum-body coordinate frame, which originates from O_h with axis z_2 pointing downward along the pendulum rod O_hO_t. After decomposing the 2-dimesional pendulum-like oscillation into ones in the directions of axes X and Y, the transition matrix R from $O_hx_2y_2z_2$ to $O_hx_1y_1z_1$ is obtained as follows:

$$\boldsymbol{R}=\begin{bmatrix}\cos\theta_y & \sin\theta_x\sin\theta_y & \cos\theta_x\sin\theta_y\\ 0 & \cos\theta_x & -\sin\theta_x\\ -\sin\theta_y & \sin\theta_x\cos\theta_y & \cos\theta_x\cos\theta_y\end{bmatrix}. \tag{1}$$

Suppose that the position vector of the suspension point O_h in the coordinate frame of $OXYZ$ and the pendulum mass O_t in the coordinate frame of $O_hx_2y_2z_2$ are presented with

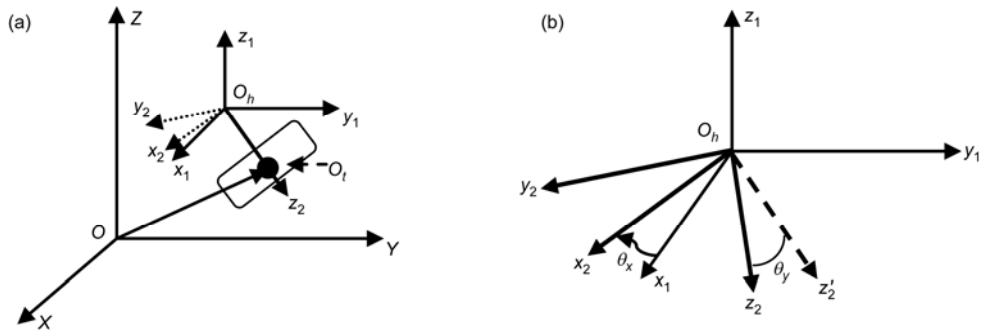

Figure 2 Coordinates of the pendulum model and decomposition of oscillation angle. (a) Coordinates of the pendulum model; (b) decomposition of oscillation angle.

$\boldsymbol{r}_h=[x,y,z]^{\mathrm{T}}$, $\boldsymbol{r}_t'=[0,0,l]^{\mathrm{T}}$, respectively. Then, the coordinate of point O_t in $O_hx_1y_1z_1$ can be calculated according to

$$\boldsymbol{r}_{ht}=\boldsymbol{R}\cdot\boldsymbol{r}_t'=\left[l\cos\theta_x\sin\theta_y,-l\sin\theta_x,l\cos\theta_x\cos\theta_y\right]^{\mathrm{T}}, \quad (2)$$

where l denotes the distance from O_h to O_t, i.e. the length of the pendulum.

Finally, we have the coordinate of O_t in the coordinate frame $OXYZ$ presented as

$$r_t=r_h+R\cdot r_t'. \quad (3)$$

The Lagrange function of the pendulum system is

$$\begin{aligned}L&=T_0-V=T_m+T_M'+T_M''-V\\&=\frac{1}{2}m\dot{\boldsymbol{r}}_h^{\mathrm{T}}\dot{\boldsymbol{r}}_h+\frac{1}{2}m_t\boldsymbol{V}_t^{\mathrm{T}}\boldsymbol{V}+\frac{1}{2}J_{x2}\omega_{x2}^2+\frac{1}{2}J_{y2}\omega_{y2}^2\\&\quad-\left(-m_tgl\cos\theta_x\cos\theta_y+(m+m_t)(z-z_0)g\right)\\&=\frac{1}{2}(m+m_t)(\dot{x}^2+\dot{y}^2+\dot{z}^2)\\&\quad+\frac{1}{6}m_tl\left[(3+\cos^2\theta_y)l\dot{\theta}_x^2+(1+3\cos^2\theta_x)l\dot{\theta}_y^2\right]\\&\quad+m_tl\left(\dot{x}\dot{\theta}_y\cos\theta_x\cos\theta_y-\dot{x}\dot{\theta}_x\sin\theta_x\sin\theta_y-\dot{y}\dot{\theta}_x\cos\theta_x\right.\\&\quad\left.-\dot{z}\dot{\theta}_x\sin\theta_x\cos\theta_y-\dot{z}\dot{\theta}_y\cos\theta_x\sin\theta_y\right)\\&\quad+m_tgl\cos\theta_x\cos\theta_y-(m+m_t)(z-z_0)g,\end{aligned} \quad (4)$$

where T_m, T_M', and T_M'' represent respectively the kinetic energy of the suspension center O_h, the translation kinetic energy of the pendulum mass O_t, and the rotational kinetic energy of the pendulum rod around the centroid of O_t, and V is the potential energy of the system, assuming the initial state of the pendulum-like oscillation as the zero-potential energy surface.

Therefore, from the Lagrange equation it can be deduced that

$$\begin{cases}\dfrac{\mathrm{d}}{\mathrm{d}t}\left(\dfrac{\partial L}{\partial\dot{\theta}_x}\right)-\dfrac{\partial L}{\partial\theta_x}=0,\\[2ex]\dfrac{\mathrm{d}}{\mathrm{d}t}\left(\dfrac{\partial L}{\partial\dot{\theta}_y}\right)-\dfrac{\partial L}{\partial\theta_y}=0.\end{cases} \quad (5)$$

Considering all the above eqs. (1)–(5), the non-linear mathematical model of the MAV pendulum-like oscillation is finally obtained as follows:

$$\begin{cases}\ddot{\theta}_x=(3\ddot{x}\sin\theta_x\sin\theta_y+3\ddot{y}\cos\theta_x+3\ddot{z}\sin\theta_x\cos\theta_y\\\quad+2l\dot{\theta}_x\dot{\theta}_y\cos\theta_x\sin\theta_y-3l\dot{\theta}_y^2\sin\theta_x\cos\theta_x-3g\sin\theta_x\cos\theta_x)\\\quad/(\cos^2\theta_y+3)l,\\\ddot{\theta}_y=(-3\ddot{x}\cos\theta_x\cos\theta_y+3\ddot{z}\cos\theta_x\sin\theta_y+6l\dot{\theta}_x\dot{\theta}_y\sin\theta_x\cos\theta_x\\\quad-l\dot{\theta}_x^2\sin\theta_y\cos\theta_y-3g\cos\theta_x\sin\theta_y)/(\cos^2\theta_x+3)l.\end{cases} \quad (6)$$

Table 1 gives the main parameters of the MAV system structure in this work.

2.2 Linearization of mathematical model

Step 1. Change the pendulum angle around axes x, y (θ_x, θ_y) to the pitch and roll angles (ϕ_x, ϕ_y) according to $\phi_x=\theta_y$, $\phi_y=-\theta_x$; then eq. (6) can be described as

$$\begin{cases}\ddot{\phi}_y=(3\ddot{x}\sin\phi_x\sin\phi_y-3\ddot{y}\cos\phi_y+3\ddot{z}\sin\phi_y\cos\phi_x\\\quad+2l\dot{\phi}_x\dot{\phi}_y\cos\phi_y\sin\phi_x-3l\dot{\phi}_x^2\sin\phi_y\cos\phi_y-3g\sin\phi_y\cos\phi_y)\\\quad/(\cos^2\phi_x+3)l,\\\ddot{\phi}_x=(-3\ddot{x}\cos\phi_y\cos\phi_x+3\ddot{z}\cos\phi_y\sin\phi_x+6l\dot{\phi}_x\dot{\phi}_y\sin\phi_y\cos\phi_y\\\quad-l\dot{\phi}_y^2\sin\phi_x\cos\phi_x-3g\cos\phi_y\sin\phi_x)/(\cos^2\phi_y+3)l.\end{cases} \quad (7)$$

Step 2. Choose the state variables $\boldsymbol{X}_e=[x,\phi_x,\dot{x},\dot{\phi}_x,y,\phi_y,\dot{y},\dot{\phi}_y,z,\dot{z},\ddot{x},\ddot{y},\ddot{z}]^{\mathrm{T}}$, and the input of the system $\boldsymbol{u}=[\ddot{x},\ddot{y}]^{\mathrm{T}}$. Expand eq. (7) into Taylor series in the vicinity of the equilibrium point, and the linear model of the pendulum-like oscillation is finally obtained as follows:

$$\begin{bmatrix}\dot{\boldsymbol{X}}_x\\\dot{\boldsymbol{X}}_y\end{bmatrix}=\begin{bmatrix}\boldsymbol{A}_x&0\\0&\boldsymbol{A}_y\end{bmatrix}\begin{bmatrix}\boldsymbol{X}_x\\\boldsymbol{X}_y\end{bmatrix}+\begin{bmatrix}\boldsymbol{B}_x&0\\0&\boldsymbol{B}_y\end{bmatrix}\begin{bmatrix}\boldsymbol{u}_x\\\boldsymbol{u}_y\end{bmatrix}, \quad (8)$$

where the state vectors $\boldsymbol{X}_x=[x,\phi_x,\dot{x},\dot{\phi}_x]^{\mathrm{T}}$, $\boldsymbol{X}_y=[y,\phi_y,\dot{y},\dot{\phi}_y]^{\mathrm{T}}$, and

$$\boldsymbol{A}_x=\begin{bmatrix}0&0&1&0\\0&0&0&1\\0&0&0&0\\0&-\dfrac{3g}{4l}&0&0\end{bmatrix},\quad\boldsymbol{A}_y=\begin{bmatrix}0&0&1&0\\0&0&0&1\\0&0&0&0\\0&-\dfrac{3g}{4l}&0&0\end{bmatrix},$$

$$\boldsymbol{B}_x=\begin{bmatrix}0\\0\\1\\-\dfrac{3}{4l}\end{bmatrix},\quad\boldsymbol{B}_y=\begin{bmatrix}0\\0\\1\\-\dfrac{3}{4l}\end{bmatrix}.$$

Table 1 Main parameters of the MAV system structure

Symbol	Value	Physical meaning
m	10 kg	suspension centre quality
m_t	20 kg	pendulum quality
l	0.86 m	pendulum length
g	9.8 m/s^2	gravity acceleration
θ_x,θ_y	–	pendulum angle around axis x, y
ϕ_x,ϕ_y	–	pitch and roll angle
a_x,a_y	–	suspension centre acceleration
u_x,u_y	–	control force on O_h

3 Design of control law

3.1 Characteristics of pendulum-like oscillation

From the linear model, the MAV pendulum-like oscillation in the directions of X and Y is no longer coupled with each other. The pendulum system can be reduced to two fourth-order subsystems, which are independent of each other. Due to similarity between matrixes A_x and A_y, we choose either of the two subsystems to analyze characteristics of the MAV pendulum-like oscillation.

Considering pendulum motion only in the direction of axis X, the state space equation of the linearized X-subsystem is presented as follows:

$$\begin{cases} \dot{\boldsymbol{X}} = \boldsymbol{AX} + \boldsymbol{BU}, \\ \boldsymbol{Y} = \boldsymbol{CX}, \end{cases} \tag{9}$$

where $\boldsymbol{X} = \left[x_1, x_2, x_3, x_4\right]^{\mathrm{T}} = \left[x, \phi_x, \dot{x}, \dot{\phi}_x\right]^{\mathrm{T}}$, and

$$\boldsymbol{A} = \begin{bmatrix} 0 & 0 & 1 & 0 \\ 0 & 0 & 0 & 1 \\ 0 & 0 & -0.6500 & 0.6500 \\ 0 & -8.547 & 0.5669 & -0.3924 \end{bmatrix},$$

$$\boldsymbol{B} = \begin{bmatrix} 0 \\ 0 \\ 1 \\ -0.872 \end{bmatrix}, \quad \boldsymbol{C} = \begin{bmatrix} 1 & 0 & 0 & 0 \\ 0 & 1 & 0 & 0 \\ 0 & 0 & 1 & 0 \\ 0 & 0 & 0 & 1 \end{bmatrix}.$$

In an actual flight, the external disturbances such as cross winds jeopardize stability of hover and stare state and lead to a considerate degradation of the surveillance performance and even result in false intelligence information. Assume there is a sudden gust, the pendulum system gets an initial state $\phi_x(0)$=0.05 rad. The inherent characteristics of the MAV pendulum-like oscillation system and the responses are given in Figure 3.

As shown in Figure 3, due to external disturbances of cross winds, which result in an initial state $\phi_x(0)$=0.05 rad, the pendulum-like oscillation occurs in MAV that is required to be stable enough to carry out hover and stare missions. However, the actual fact shown by the analysis results states clearly that the position of the suspension, denoted as x in Figure 3, does not remain in the original place but moves to another site in 20 s, which may bring about deviation from the ideal monitoring precision. Furthermore, the MAV's body swings back and forth just in the way as a pendulum does, and eventually converges to the equilibrium point after 25 s.

3.2 Control law design based on LQR

As mentioned above, the hover and stare state is inherently unstable and external disturbances would give rise to pendulum-like oscillation depicted as in Figure 3. A novel type of optimal control law based on LQR and PSO is designed in this section, which is used to eliminate the pendulum-like oscillation within the shortest duration. In this controller, the position of the suspension point x and the pendulum angle ϕ_x are the two main state variables that are controlled to keep the desired values. In order to ensure the robustness and optimality of the close loop, the LQR design technique is applied due to the fact that it has a very nice robustness property, and has been widely used in many applications.

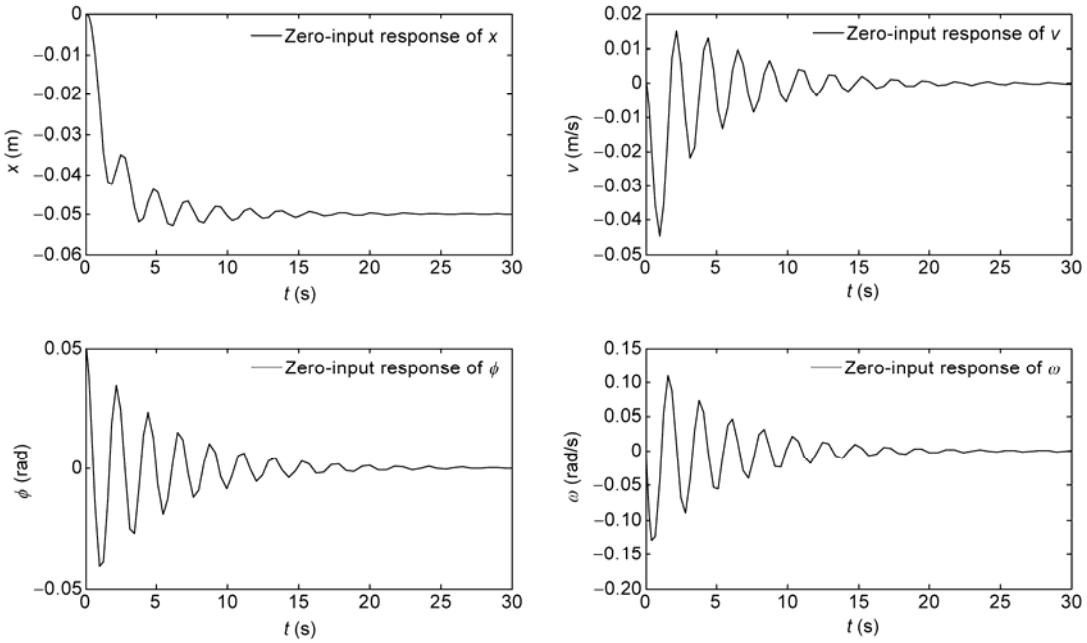

Figure 3 Responses of the MAV pendulum-like oscillation system.

The key issue of LQR controller design is how to select an appropriate control vector $u(t)$ so that the given quadratic performance index (see eq. (10)) obtains the minimum value. It is proved that the performance index can reach its minimum by the designed linear control law in eq. (11).

$$\boldsymbol{J}=\int_0^{\infty}\left(\boldsymbol{X}^{\mathrm{T}}\boldsymbol{Q}\boldsymbol{X}+\boldsymbol{u}^{\mathrm{T}}\boldsymbol{R}\boldsymbol{u}\right)\mathrm{d}t, \tag{10}$$

$$\boldsymbol{u}(t)=-\boldsymbol{K}\boldsymbol{X}(t)=\boldsymbol{R}^{-1}\boldsymbol{B}^{\mathrm{T}}\boldsymbol{P}\boldsymbol{X}(t), \tag{11}$$

and the optimal matrix P can be calculated from the following algebraic Riccati equation:

$$\boldsymbol{A}^{\mathrm{T}}\boldsymbol{P}+\boldsymbol{P}\boldsymbol{A}-\boldsymbol{P}\boldsymbol{B}\boldsymbol{R}^{-1}\boldsymbol{B}^{\mathrm{T}}\boldsymbol{P}+\boldsymbol{Q}=0. \tag{12}$$

Taking all factors into account, including the performance of the control system and restrictions on the total energy consumed, we can define matrixes $\boldsymbol{Q}$ and $\boldsymbol{R}$ in the form of $\boldsymbol{Q}$=diag(q_{11}, q_{22}, 0, 0), and R=1, in which parameters q_{11} and q_{22} are crucial for a splendid dynamic response. As a result, the proposed algorithm takes advantages of PSO's high operating efficiency, fast convergence speed and model simplicity to search the appropriate parameter setting of the LQR control law design approach.

Let input $\boldsymbol{u}$ be the control force acting on the suspension center, and the corresponding pendulum-holding back control law from the LQR be described as follows:

$$\boldsymbol{u}=-\boldsymbol{K}\boldsymbol{X}=-\left(k_1x_1+k_2x_2+k_3x_3+k_4x_4\right), \tag{13}$$

where $\boldsymbol{K}$ denotes the feedback parameter vector obtained for the LQR, and $\boldsymbol{X}$ denotes the state vector of the system, i.e., the position of the suspension center, the angle of the pendulum, the speed of the suspension center, and the angular velocity of the pendulum.

The PSO based LQR controller for prohibiting MAV pendulum-like oscillation of the hover and stare state in presence of external disturbances can be illustrated with Figure 4.

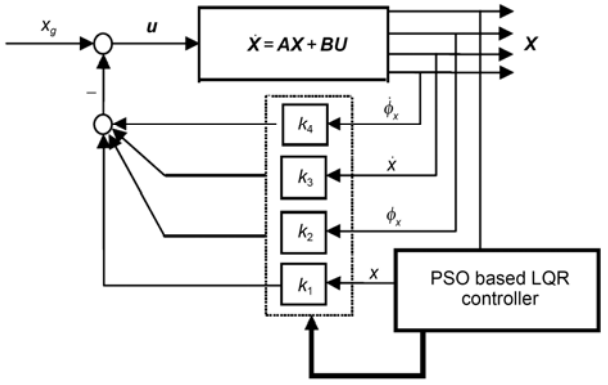

Figure 4 Structure of pendulum-like oscillation control system.

3.3 Parameter optimization based on PSO

3.3.1 The principle of PSO

PSO algorithm was firstly proposed by Kennedy and Eberhart in 1995 [14], which is one of the newly bio-inspired computation techniques for solving the complex optimization problems. The individual in the population, called the particle, dynamically adjusts its position according to its velocity influenced by its own experience and the experience of the population. PSO makes use of a velocity vector to update the current position of each particle in swarm. The position of each particle is updated based on the social behavior of individuals and the whole swarm. The scheme for updating the position vector is shown as follows:

$$\boldsymbol{x}_{k+1}^{i}=\boldsymbol{x}_{k}^{i}+\boldsymbol{v}_{k+1}^{i}\Delta t, \tag{14}$$

where $\boldsymbol{x}_{k+1}^{i}$ denotes the position of particle i at iteration k+1, and $\boldsymbol{v}_{k+1}^{i}$ denotes the corresponding velocity vector.

The scheme for updating the velocity vector of each particle depends on the particular PSO algorithm under consideration. In this work, the adopted scheme can be described as follows:

$$\boldsymbol{v}_{k+1}^{i}=\omega\boldsymbol{v}_{k}^{i}+c_1r_1\frac{p^{i}-x_k^{i}}{\Delta t}+c_2r_2\frac{p_k^{g}-x_k^{i}}{\Delta t}, \tag{15}$$

where r_1 and r_2 are random numbers between 0 and 1, p_i is the best position found by particle i so far and p_g^k is the best position in the swarm at time k. There are also three problem dependent parameters, the inertia of the particle (ω), and two trust parameters c_1 and c_2, which indicate how much confidence the current particle has in itself (c_1) and how much confidence it has in the swarm (c_2).

3.3.2 Key settings for PSO

1) Fitness function f. The fitness function f chosen in the LQR controller can be described as follows:

$$f=\frac{1}{\int_0^{\infty}(\boldsymbol{X}^{\mathrm{T}}\boldsymbol{Q}\boldsymbol{X}+\boldsymbol{u}^{\mathrm{T}}\boldsymbol{R}\boldsymbol{u})\mathrm{d}t}, \tag{16}$$

where

$$\boldsymbol{u}=-(k_1x_1+k_2x_2+k_3x_3+k_4x_4),$$
$$\boldsymbol{K}=[k_1,k_2,k_3,k_4]=\mathrm{lqr}(\boldsymbol{A},\boldsymbol{B},\boldsymbol{Q},\boldsymbol{R}),$$
$$\boldsymbol{Q}=\mathrm{diag}(q_{11},q_{22},0,0).$$

2) Inertia weight ω. The inertia weight ω controls the exploration properties of the algorithm, with a larger value facilitating a more global behavior and a smaller value facilitating a more local behavior, thus results of the algorithm depend largely on ω selection. Generally, there are two ways to choose the inertia weight, namely constant ω and time-variant ω. Prof. Shi suggested using $0.8<\omega<1.4$, which

starts with bigger ω values (a more global search behavior) that is dynamically reduced (a more local search behavior) during the optimization [15]. In this work, ω can be declined linearly from 1.4 to 0.8 in the former 75% phylogenetic scale, and keeps constant in the rest of the time.

3) Population size m. According to the scale of the exact optimization problem, m is set between 40 and 150. Here we choose m=100.

4) Acceleration constants c_1 and c_2. Ref. [15] suggests c_1=c_2=2, and the mean value of the stochastic multipliers of eq. (14) be equal to 1. Related work showed that each particle putting slightly more trust in the swarm (a larger c_2 value) and slightly less trust in itself (a smaller c_1 value) seems to act better for the structural design problems [16]. According to experiences, we choose c_1=1.8 and c_2=1.3.

4 Experimental results

Assume the designed MAV to execute a surveillance mission using the hover and stare mode in the actual flight. Considering external disturbances and taking the cross winds for example, the system gets an initial state x=[0, 0.05, 0, 0], which gives rise to pendulum oscillation without an appropriate control.

With the proposed controller described in Figure 4 and experimental settings given in Section 3, the control parameters which include the optimal weight matrix $\boldsymbol{Q}$ and the resulting feedback vector $\boldsymbol{K}$ are obtained as shown in Table 2.

Figure 6 shows the evolution curve of the PSO algorithm for optimizing the weight parameters of the designed LQR controller.

The zero-input responses of the MAV pendulum-like oscillation is shown with Figure 7. The initial pendulum angle is 0.05 rad, which is brought about by cross winds in the actual flight environment.

Table 2 Control parameters of the PSO based LQR approach

Parameter	Optimized value
Matrix $\boldsymbol{Q}$	Diag(245.6, 250.3, 0, 0)
Feedback vector $\boldsymbol{K}$	[15.6709 −17.1806 8.6616 2.2921]

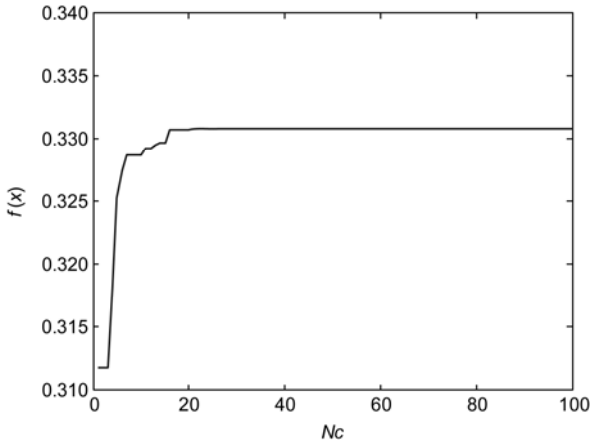

Figure 6 The average evolution curve of the PSO.

Compared with the responses without control in Figure 3, it is obvious from the dynamic behaviors of x and ϕ_x in Figure 7 that the closed loop can eliminate the pendulum-like oscillation, and the state converges to the equilibrium point within an average time of 6 s.

Furthermore, considering a constant interference force acting upon the pendulum system, the interference value is

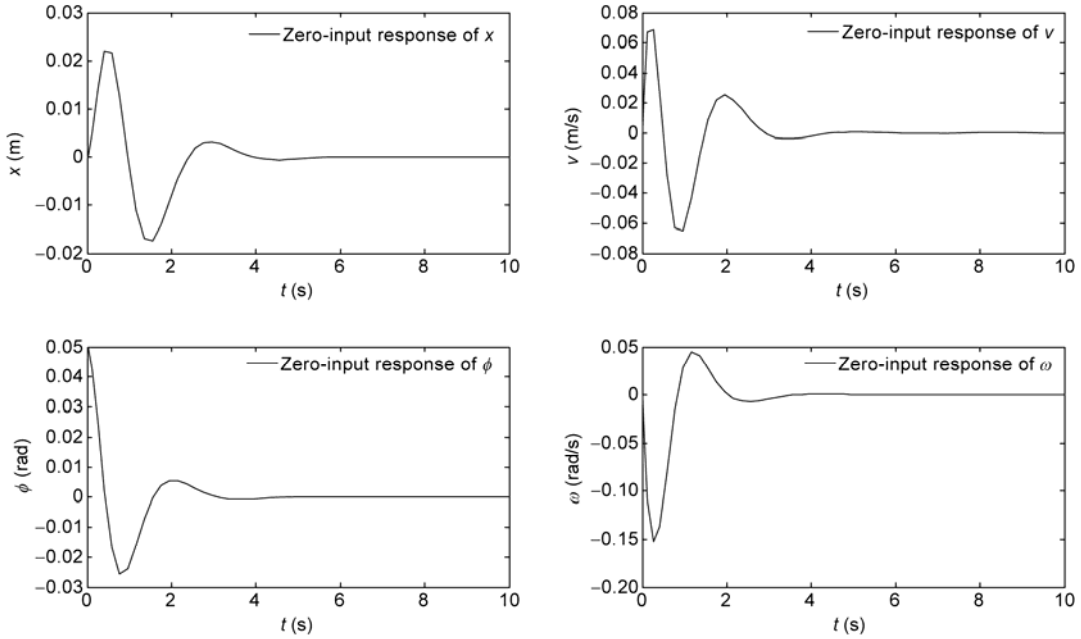

Figure 7 The zero-input responses of the MAV pendulum-like oscillation system.

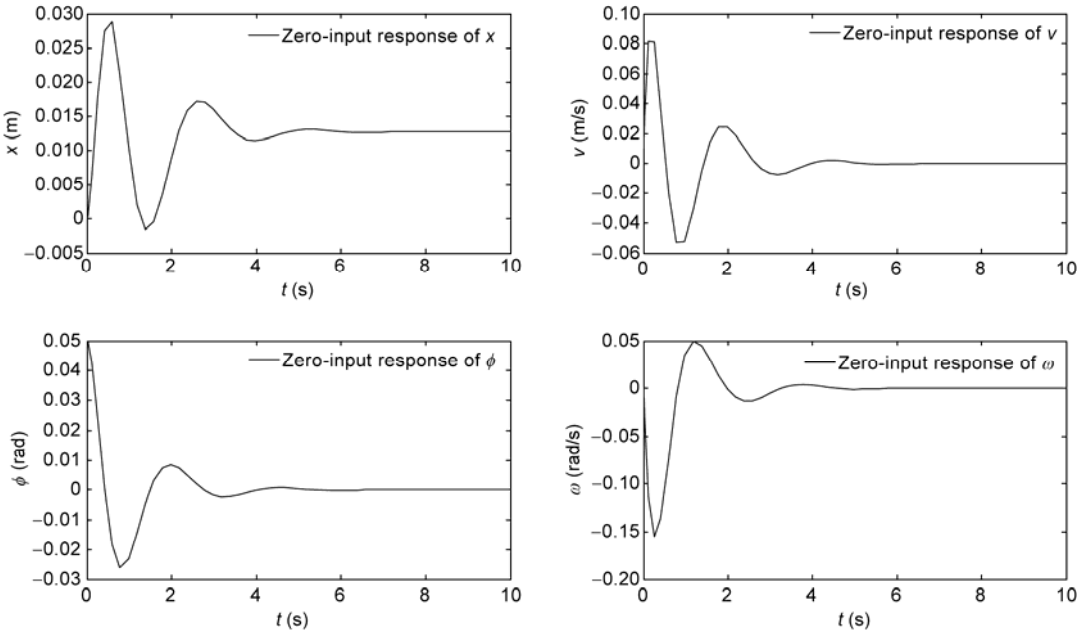

Figure 8 Responses of the MAV pendulum system with a constant disturbance.

setted as 0.2 m/s^2, and the control framework and relative parameters remain the same as mentioned above in Figure 4 and Table 2. The resulting responses are given in Figure 8.

From Figure 8, it is obvious that the PSO based LQR controller can eliminate the interference of the constant disturbance and the initial state within 6 s. The MAV is stabilized to a state of x=[0.0128, 0, 0, 0], indicating that the PSO based LQR controller is robust to external disturbances.

5 Conclusions

Hover stability is the key issue for MAVs which are designed to carry out surveillance and reconnaissance missions. However, the pendulum-like oscillation caused by uncertainty and external disturbances badly jeopardize the performance of hover and stare, resulting in blurred images or even MAV's overturning. This paper mainly focuses on the control issue of pendulum-like oscillation in the MAV's hover and stare state in the presence of external disturbances. A novel type of PSO based LQR controller for stabilizing the pendulum-like oscillation is developed, which can enhance the MAV's surveillance performance efficiently. A series of comparative results have verified the feasibility and effectiveness of our approach.

This work was supported by the National Natural Science Foundation of China (Grant Nos. 61273054, 60975072, 60604009), the Program for New Century Excellent Talents in University of China (Grant No. NCET-10-0021), the Aeronautical Foundation of China (Grant No. 20115151019), and the Opening Foundation of State Key Laboratory of Virtual Reality Technology and Systems of China (Grant No. VR-2011-ZZ-01).

1 Eric J, Michael T. Modeling, control, and flight testing of a small-ducted fan aircraft. J Guid, Contr, Dynam, 2006, 29: 769–779
2 Richard B. Latest unmanned vehicle show features both innovative new vehicles and miniaturization. Industr Robot Int J, 2009, 36: 13–18
3 Office of the Secretary of Defense. Unmanned aircraft systems roadmap 2005–2030. Washington DC, 2005
4 Duan H B, Shao S, Su B W, et al. New development thoughts on the bio-inspired intelligence based control for Unmanned Combat Aerial Vehicle. Sci China Tech Sci, 2010, 53: 2025–2031
5 Li P, Duan H B. Path planning of Unmanned Aerial Vehicle based on improved gravitational search algorithm. Sci China Tech Sci, 2012, 55: 2712–2719
6 Duan H B, Zhang X Y, Wu J, et al. Max-Min Adaptive ant colony optimization approach to multi-UAVs coordinated trajectory re-planning in dynamic and uncertain environments. J Bionic Eng, 2009, 6: 161–173
7 Christian S, Oliver M, Natalie F, et al. Using natural features for vision based navigation of an indoor-VTOL MAV. Aerosp Sci Tech, 2009, 13: 349–357
8 Tsai B J, Fu Y C. Design and aerodynamic analysis of a flapping-wing micro aerial vehicle. Aerosp Sci Tech, 2009, 13: 383–392
9 Thomas R, Mustapha O, Thierry L M. Longitudinal modeling and control of a flapping-wing micro aerial vehicle. Contr Eng Pract, 2010, 18: 679–690
10 Pflimlin J M, Binetti P, Soueres P, et al. Modeling and attitude control analysis of a ducted-fan micro aerial vehicle. Contr Eng Pract, 2010, 18: 209–218
11 Pu H Z, Zhen Z Y, Wang D B, et al. Improved particle swarm optimization algorithm for intelligently setting UAV attitude controller parameters. Trans Nanjing Univ Aeron & Astro, 2009, 26: 52–57
12 Pu H Z, Zhen Z Y, Wang D B. Modified shuffled frog leaping algorithm for optimization of UAV flight controller. Int J Int Comp Cybern, 2011, 4: 5–39
13 Osgar O, Paul G, Daniel I. Nondimensional modeling of ducted-fan aerodynamics. J Aircraft, 2012, 49: 126–140
14 Kennedy J, Eberhart R C. Particle swarm optimization. In: Proceedings of the 1995 IEEE International Conference on Neural Networks, Perth, Australia, 1995. 1942–1948
15 Shi Y H, Eberhart R C. Parameter selection in particle swarm optimization. Lect Note Comp Sci, 1998, 1447: 591–600
16 Gerhard V. Particle swarm optimization. In: Proceedings of the 43rd AIAA/ASME/ASCE/AHS/ASC Structures, Structural Dynamics, and Materials Conference, Denver, Colorado, 2002. 22–25